

GradMAP: Faster Layer Pruning with Gradient Metric and Projection Compensation

Hao Liu^{1,2*}, Guangyan Li^{1,2*}, Wensheng Zhang³, Yongqiang Tang^{1†}

¹ Institute of Automation, Chinese Academy of Sciences,

² School of Artificial Intelligence, University of Chinese Academy of Sciences,

³ Guangzhou University

Abstract

Large Language Models (LLMs) exhibit strong reasoning abilities, but their high computational costs limit their practical deployment. Recent studies reveal significant redundancy in LLMs layers, making layer pruning an active research topic. Layer pruning research primarily focuses on two aspects: measuring layer importance and recovering performance after pruning. Unfortunately, the present works fail to simultaneously maintain pruning performance and efficiency. In this study, we propose GradMAP, a faster layer pruning method with **Gradient Metric And Projection compensation**, which consists of two stages. In the first stage, we introduce a novel metric based on gradient magnitudes, enabling a global assessment of layer importance. Note that, it requires only a single backward propagation step per pruning decision, substantially enhancing pruning efficiency. In the second stage, we first analyze the layers with the largest mean shift resulting from pruning, and then incorporate a simple yet effective projection compensation matrix to correct this drift in one step. In this way, the degradation of model performance caused by layer pruning is effectively alleviated. Extensive experiments show that GradMAP outperforms previous layer pruning methods in both pruning speed (achieving an average $4\times$ speedup) and performance.

1 Introduction

Large Language Models (LLMs) (Brown et al., 2020; Achiam et al., 2023; Touvron et al., 2023; Chiang et al., 2023) have demonstrated remarkable capabilities across various domains (Hendrycks et al., 2020a; Chiang et al., 2024). However, deploying these models remains a significant challenge due to their huge

*Equal contribution.

†Corresponding author: yongqiang.tang@ia.ac.cn

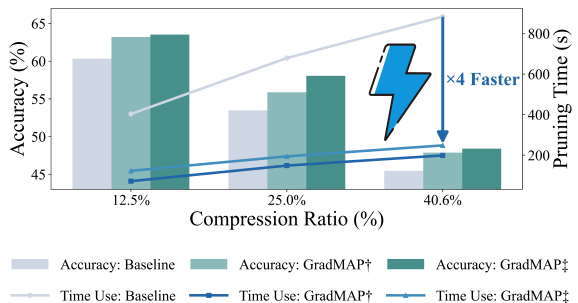


Figure 1: Comparison of pruning time and accuracy across different methods on the Vicuna-7B.

computational and memory demands. Numerous techniques have been proposed to compress transformer-based models, including pruning (Han et al., 2015a; Xia et al., 2022; Kurtic et al., 2022), low-rank approximation (Noach and Goldberg, 2020; Li et al., 2024), quantization (Frantar et al., 2023; Yao et al., 2022; Dettmers et al., 2023), and knowledge distillation (Saha et al., 2023). Quantization reduces memory usage but depends on specialized hardware. Knowledge distillation compresses models but requires additional training. Low-rank approximation reduces size but demands further optimization. In contrast, pruning removes redundant parameters without retraining, offering an effective way.

Previous work mainly focuses on pruning the dense matrices in LLMs, which leads to two main directions: unstructured pruning and structured pruning. Unstructured pruning methods, such as Wanda (Sun et al., 2023), remove individual weights based on their importance. While effective, unstructured pruning modifies the internal weight matrices, making it more challenging to deploy pruned models in real-world systems. On the other hand, structured pruning methods, such as LLM-Pruner (Ma et al., 2023), remove groups of neurons based on their connectivity, achieving significant model compression without compromis-

ing performance. Building upon structured pruning, layer pruning further reduces model complexity by removing entire layers, rather than individual weights or neurons. This approach does not alter the internal weight structure, improving computational efficiency (Song et al., 2024) and easier to integrate into existing model pipelines (Chen et al., 2024). Recently, due to its direct impact on reducing parameter scale, layer pruning has become a popular focus in LLMs compression research.

Existing layer pruning research can be viewed through two lenses: (1) how to quantify a layers importance; (2) how to compensate the performance lost once layers are pruned. As for the *importance measurement* of layers, a straightforward idea is to compare a layers input and output representations with cosine similarity (e.g., Short-GPT (Men et al., 2025) and Laco (Yang et al., 2024b)). Such metric only measures the similarity of hidden states and does not consider how a layer contributes to the task performance, thus leading to potential inaccuracies in identifying truly unimportant layers. To remedy this issue, SLEB (Song et al., 2024) and BlockPruner (Zhong et al., 2024) progressively mask each layer or sub-layer and then calculate the resulting loss change to identify the non-essential layers. However, their evaluation loop incurs substantial computational overhead, limiting their effectiveness and efficiency in practical pruning of LLMs. It is worthy noting that, the methods mentioned above merely remove unimportant layers in a rough manner, without any extra compensation mechanisms, resulting in suboptimal performance. More recently, an increasing body of research has recognized the necessity of *performance recovery* after layers pruning. For instance, LLM-Streamline (Chen et al., 2024) trains a lightweight layers to recover performance without significantly increasing the model size. UIDL (Gromov et al., 2024), on the other hand, restores accuracy by combining pruning with conventional fine-tuning techniques such as QLoRA. While effective, these approaches typically rely on a large number of calibration samples and demand considerable computational resources and fine-tuning time, making them less efficient.

To address the noted challenges, we propose GradMAP, a faster layer pruning method with **Gradient Metric And Projection compensation**. Previous studies have demonstrated that gradient information inherently captures parameter sensitivity and the influence on task optimiza-

tion (Molchanov et al., 2016; Singh and Alistarh, 2020). Building on this insight, we propose a layer importance metric based on global gradient magnitudes to directly quantify each layers contribution to model performance. Moreover, to enable rapid recovery of model performance after pruning, we analyze the shift in the after-pruning activations first-order moments and introduce a gradient-free projection compensation matrix. This matrix aligns the pruned models outputs with those of the original model, effectively compensating for the performance degradation with minimal computational overhead. In summary, GradMAP operates in two stages: In the first stage, we introduce a novel importance metric based on global gradient magnitudes, allowing precise identification of unimportant layers. In the second stage, we analyze the shift in the first-order moment of activations caused by pruning and mitigate it by training a projection compensation matrix that aligns the after-pruning outputs with their original counterparts, thereby recovering performance with minimal overhead. As shown in Figure 1, our method prunes faster and performs better than prior approaches. Our contributions can be summarized as follows:

- We propose GradMAP, a faster and more effective layer pruning method. To better quantify the importance of each layer, we introduce a novel metric based on global gradient magnitudes. Additionally, we propose a projection compensation matrix to restore model performance after pruning.
- The projection compensation matrix we propose can be seamlessly integrated into existing layer pruning frameworks, offering an effective means of recovering model performance while introducing minimal computational overhead. This integration can significantly enhance the pruning efficiency of current methods.
- We evaluate the performance of the compressed model through zero-shot perplexity on the WikiText2, PTB and C4 datasets, as well as zero-shot task classification on common-sense reasoning datasets. Our method not only achieves an average pruning speed improvement of $4\times$, but also outperforms existing layer pruning methods.

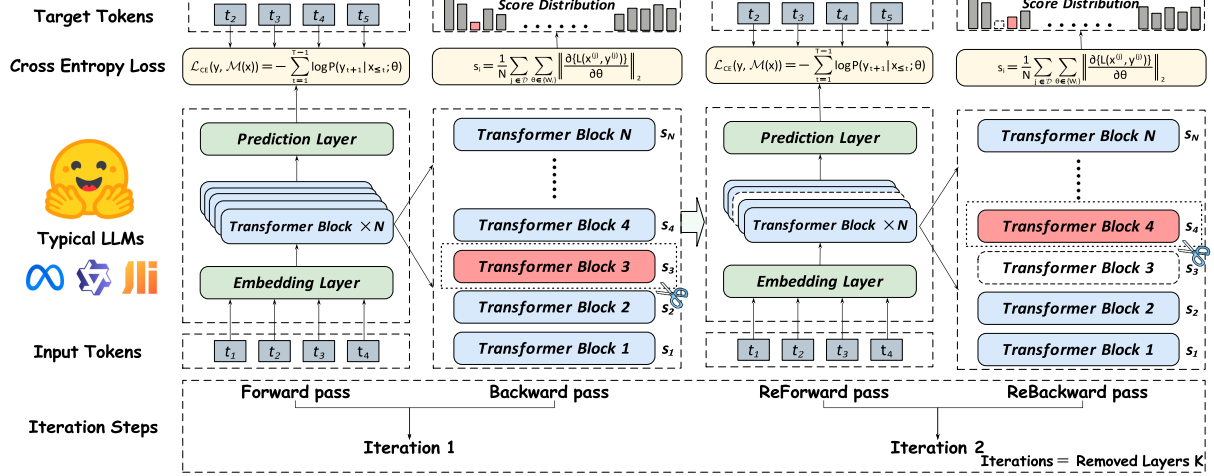


Figure 2: The Stage 1 of GradMAP introduces a novel gradient-based metric for estimating layer importance in LLMs, which quantifies each layer’s contribution by analyzing gradient magnitudes. This metric enables the iterative identification and pruning of unimportant layers.

2 Methodology

2.1 Problem Formulation

Most Large Language Models (LLMs) are built on the Transformer architecture (Vaswani et al., 2017), where each layer consists of two key components: a self-attention layer and a feed-forward network (FFN) layer. Given the hidden representation $\mathbf{H}_{(i-1)}$ from layer $(i-1)$, the i -th layers transformation is:

$$\mathbf{H}_i = \text{FFN}(\text{Self-Attn}(\mathbf{H}_{(i-1)})), \quad (1)$$

where Self-Attn computes dependencies between tokens using the attention mechanism, and FFN applies non-linear transformations. The standard design stacks L layers to refine representations.

Prior studies (Song et al., 2024; Zhong et al., 2024; Men et al., 2025) have demonstrated that LLMs contain considerable redundancy across layers. These findings have led to a common layer pruning paradigm: assess each layers importance, remove the unimportant ones, and optionally fine-tune the model to recover accuracy. In this study, we formalize layer pruning as:

Importance Scoring: Compute layer-wise importance scores:

$$s_i = \Phi(\theta_i; \mathcal{D}), \quad (2)$$

where θ_i can represent either model parameters (Song et al., 2024) or hidden states \mathbf{H}_i (Men et al., 2025), and \mathcal{D} denotes a calibration dataset.

Adaptive Selection and Fine-tuning: Determine a ranking permutation $\pi = \text{argsort}(s_i)$ such

that $s_{\pi(1)} \geq s_{\pi(2)} \geq \dots \geq s_{\pi(L)}$. The pruned model retains the top $(L - K)$ layers:

$$\mathcal{S} = \{\pi(1), \pi(2), \dots, \pi(L - K)\}, \quad (3)$$

where L denotes the total number of layers, and K represents the number of pruned layers.

Optionally, fine-tune the pruned model on a small calibration dataset \mathcal{D} . The updated model parameters are obtained by minimizing the loss:

$$\theta^* = \arg \min_{\theta} \mathcal{L}(\mathcal{D}; \theta). \quad (4)$$

2.2 The Proposed GradMAP

Building on the standard layer pruning framework, we propose GradMAP. In Stage 1, GradMAP quantifies each layer’s contribution to model performance by analyzing the gradients propagated through the network using calibration data. Unlike conventional methods that rely solely on hidden state similarity, this approach provides a more precise identification of redundant layers, ensuring that pruning minimally impacts model performance. Furthermore, it is important to highlight that although our approach utilizes gradients, we do not perform any training or parameter updates on the LLM itself. In Stage 2, we introduce a projection compensation matrix to address the performance degradation caused by pruning. Notably, this stage does not require any further gradient computations, making it highly efficient in terms of both time and computational resources.

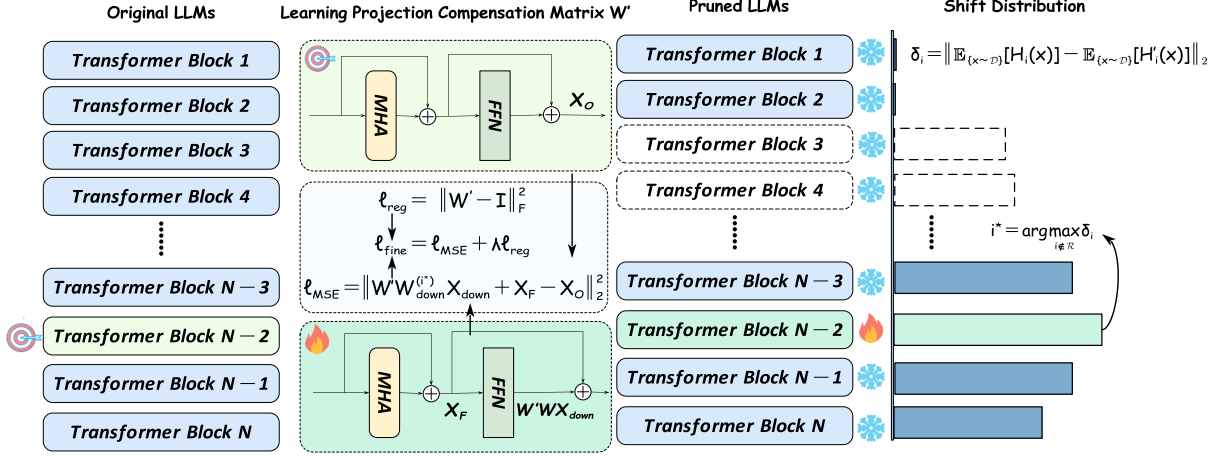


Figure 3: The Stage 2 of GradMAP. To mitigate capacity loss, we introduce a learnable projection compensation matrix that optimizes reconstruction on a small calibration dataset.

Stage 1: Measuring Layer Importance via Gradient Magnitude. Given a pre-trained language model \mathcal{M} parameterized by θ with L layers, processing the input sequence $\mathbf{x} = [x_1, \dots, x_T]$ and generating the target sequence $\mathbf{y} = [y_1, \dots, y_T]$. The cross-entropy loss is defined as:

$$\mathcal{L}_{\text{CE}}(\mathbf{x}, \mathbf{y}) = - \sum_{t=1}^{T-1} \log P(y_{t+1} | \mathbf{x}_{\leq t}; \theta). \quad (5)$$

To estimate layer-wise importance, we utilize a small calibration dataset $\mathcal{D} = \{(\mathbf{x}^{(j)}, \mathbf{y}^{(j)})\}_{j=1}^N$ containing N examples sampled from Wikipedia. Given the cross-entropy loss \mathcal{L}_{CE} defined in Eq. (5), we first perform a forward pass on each input-output pair $(\mathbf{x}^{(j)}, \mathbf{y}^{(j)}) \in \mathcal{D}$ to compute the loss value $\mathcal{L}_{\text{CE}}(\mathbf{x}^{(j)}, \mathbf{y}^{(j)})$. And we then apply backpropagation to obtain the gradients of this loss with respect to all parameters in each layer.

Specifically, for each layer indexed by $i = 1, \dots, L$, we define its trainable parameter set \mathcal{W}_i to include all learnable tensors within the layer. For each calibration sample, we compute the total gradient magnitude of layer index i by summing the L_2 norms of the gradients of all tensors $\theta \in \mathcal{W}_i$:

$$G_i^{(j)} = \sum_{\theta \in \mathcal{W}_i} \left\| \frac{\partial \mathcal{L}_{\text{CE}}(\mathbf{x}^{(j)}, \mathbf{y}^{(j)})}{\partial \theta} \right\|_2. \quad (6)$$

The final importance score for layer i is then defined as the average of $G_i^{(j)}$ over all samples:

$$s_i = \frac{1}{N} \sum_{j \in \mathcal{D}} \sum_{\theta \in \mathcal{W}_i} \left\| \frac{\partial \mathcal{L}_{\text{CE}}(\mathbf{x}^{(j)}, \mathbf{y}^{(j)})}{\partial \theta} \right\|_2. \quad (7)$$

As illustrated in Figure 2, layers with lower importance scores contribute less to the models learning and thus can be pruned with minimal impact on performance. Specifically, we iteratively remove layers with lower importance scores until the target number of layers $L - K$ is reached.

Stage 2: Performance Recovery via Projection Compensation Matrix. To mitigate the performance degradation caused by pruned layers, GradMAP introduces a compensation mechanism. Specifically, we propose an adaptive compensation strategy that approximates the functionality of pruned layers using a learned transformation matrix applied to remaining layers. This method can seamlessly integrates with existing pruning techniques, and enhances model performance with minimal computational overhead.

As illustrated in Figure 3, we first quantify the drift in the first-order moment (mean) between the outputs of the retained layers before and after pruning. We then identify the layer exhibiting the largest drift and introduce a learnable projection compensation matrix W' to compensate the mismatch. Formally, consider the original LLM \mathcal{M} with L layers indexed by $i = 1, \dots, L$. After pruning a subset of layers with indices $\mathcal{R} = \{r_1, r_2, \dots, r_K\}$, let $\mathbf{H}_i(\mathbf{x})$ and $\mathbf{H}'_i(\mathbf{x})$ denote the outputs of layer i in the original and pruned models, respectively. For each retained layer ($i \notin \mathcal{R}$), we quantify its mean drift before and after pruning on the calibration dataset \mathcal{D} as:

$$\delta_i = \left\| \mathbb{E}_{\mathbf{x} \sim \mathcal{D}} [\mathbf{H}_i(\mathbf{x})] - \mathbb{E}_{\mathbf{x} \sim \mathcal{D}} [\mathbf{H}'_i(\mathbf{x})] \right\|_2. \quad (8)$$

Although it is possible to apply compensation to

Algorithm 1 The pseudo-code of GradMAP

Input: Calibration dataset $\mathcal{D} = \{(\mathbf{x}^{(j)}, \mathbf{y}^{(j)})\}_{j=1}^N$,
Original LLM \mathcal{M} , Target layer count $L - K$
Output: Pruned LLM \mathcal{M}'

- 1: **Stage 1: Gradient-Based Layer Pruning**
- 2: Initialize the set of removed layers $\mathcal{R} = \emptyset$
- 3: **while** $|\mathcal{R}| < K$ **do**
- 4: **for** each layer $i \notin \mathcal{R}$ **do**
- 5: Compute the loss by Eq.(5);
- 6: Compute the gradient by Eq.(6);
- 7: Compute the importance score by Eq.(7);
- 8: **end for**
- 9: Find worst layer: $\ell^* = \arg \min s_i$;
- 10: Update removal set: $\mathcal{R} \leftarrow \mathcal{R} \cup \{\ell^*\}$;
- 11: Remove layer ℓ^* : $\mathcal{M} \leftarrow \text{Prune}(\mathcal{M}, \ell^*)$;
- 12: **end while**
- 13: **Stage 2: Projection Compensation Matrix Learning**
- 14: Compute the mean drift by Eq.(8);
- 15: Identify the layer with largest drift by Eq.(9);
- 16: Extract the down-projection matrix $\mathbf{W}_{down}^{(i^*)}$;
- 17: Learn \mathbf{W}' by Eq.(10);
- 18: Construct final model: $\mathcal{M}' \leftarrow \mathbf{W}' \mathbf{W}_{down}^{(i^*)}$.

the Top- Z layers with the largest drift, we find that increasing Z does not consistently improve performance and instead unnecessarily increases computational overhead (see The Ablation Studies Section). Therefore, we adopt a simple yet effective approach by selecting only the largest drift layer for compensation, i.e., $Z = 1$:

$$i^* = \arg \max_{i \notin \mathcal{R}} \delta_i. \quad (9)$$

To compensate for this maximal drift, we first extract the down-projection matrix $\mathbf{W}_{down}^{(i^*)} \in \mathbb{R}^{d \times k}$ from layer i^* that exhibits the largest drift. Then, we introduce a projection compensation matrix $\mathbf{W}' \in \mathbb{R}^{d \times d}$, trained specifically to align the after-pruning output distribution of layer i^* with its before-pruning counterpart. The combined optimization objective is defined as:

$$\mathbf{W}' = \arg \min_{\mathbf{W}'} \mathbb{E}_{(\mathbf{x}, \mathbf{y}) \sim \mathcal{D}} [\mathcal{L}_{\text{MSE}} + \mathcal{L}_{\text{reg}}], \quad (10)$$

where the mean squared error (MSE) term is

$$\mathcal{L}_{\text{MSE}} = \left\| \mathbf{W}' \mathbf{W}_{down}^{(i^*)} \mathbf{X}_{down} + \mathbf{X}_F - \mathbf{X}_O \right\|_2^2 \quad (11)$$

and the regularization term is

$$\mathcal{L}_{\text{reg}} = \lambda \left\| \mathbf{W}' - \mathbf{I} \right\|_F^2. \quad (12)$$

Here, \mathbf{X}_O denotes the output activations before pruning, \mathbf{X}_F represents the input activations to the FFN sub-layer after pruning, and \mathbf{X}_{down} is the input to the down-projection matrix in the FFN sub-layer after pruning. The regularization term constrains \mathbf{W}' toward the identity matrix, minimizing distortion of the original representations.

For efficient deployment and inference, the calibrated down-projection weight matrix $\hat{\mathbf{W}}_{down}^{(i^*)}$ is then obtained by re-parameterizing the original weights $\mathbf{W}_{down}^{(i^*)}$ as:

$$\hat{\mathbf{W}}_{down}^{(i^*)} = \mathbf{W}' \mathbf{W}_{down}^{(i^*)}. \quad (13)$$

Discussion. The optimization procedure of GradMAP is summarized in Algorithm 1. Compared to prior methods, GradMAP achieves superior efficiency from both the pruning and compensation stages. Firstly, the proposed importance metric in Stage 1 significantly reduces computational complexity compared to existing pruning methods. GradMAP uses gradient magnitude as a direct and differentiable metric for importance, enabling each pruning decision to be made with just one forward-backward pass. Hence, our method scales linearly rather than quadratically, dramatically accelerating the pruning procedure. Secondly, Stage 2 introduces a simple yet effective projection compensation matrix whose training is inherently lightweight. Unlike previous methods that require compensating or fine-tuning every pruned layer, our projection matrix targets only the layer with the largest activation drift after pruning. This focused approach substantially reduces computational requirements, further enhancing the overall efficiency. In addition, we provide a theoretical analysis in Appendix B.

3 Experimental Setup

We evaluated GradMAP on several large language models, including LLaMA2-7B and 13B (Touvron et al., 2023), Vicuna-7B (Chiang et al., 2023), LLaMA3.1-8B (Grattafiori et al., 2024), Baichuan2-7B (Yang et al., 2023), and Qwen2.5-7B (Yang et al., 2024a). During the model compression process, we randomly extract 128 samples from Wikipedia as calibration data, and each sample is consisted of 128 tokens. For perplexity evaluation, we used three benchmark datasets: PTB (Marcus et al., 1993), WikiText-2 (Merity et al., 2016), and C4 (Raffel et al., 2020). For

Ratio	Method	Average Accuracy↑			PPL↓			Pruning Time↓		
		LLaMA2-7B	LLaMA2-13B	Vicuna-7B	LLaMA2-7B	LLaMA2-13B	Vicuna-7B	LLaMA2-7B	LLaMA2-13B	Vicuna-7B
0%	Dense	66.79	69.31	66.85	12.18	10.98	16.23	–	–	–
12.50%	SLEB	60.87	60.60	62.79	16.68	14.63	21.68	503.98	1638.51	506.11
	ShortGPT*	62.32	64.14	63.21	16.85	14.78	21.63	519.33	1682.42	523.34
	MKA	57.80	59.82	58.31	213.40	253.40	227.19	179.55	381.04	181.01
	GradMAP	62.54	64.34	63.21	15.86	14.78	20.16	71.40	185.06	71.77
	GradMAP	62.54	64.39	63.52	15.49	14.55	20.12	122.20	261.65	122.79
25.00%	SLEB	55.96	57.79	54.88	21.76	18.83	31.66	801.58	2464.18	902.32
	ShortGPT*	54.19	58.97	52.98	33.31	23.85	48.37	831.16	2552.41	923.20
	MKA	53.44	54.26	52.56	877.70	1252.39	1140.32	182.58	542.56	199.16
	GradMAP	56.08	59.33	55.88	21.50	19.39	28.49	123.42	299.30	148.63
	GradMAP	58.59	59.62	58.06	20.56	18.53	27.56	169.42	368.30	194.13
40.63%	SLEB	42.40	46.77	46.74	103.61	44.65	85.23	1201.52	3411.58	1204.44
	ShortGPT*	44.87	49.34	42.46	384.95	60.67	649.73	1244.63	3530.80	1247.18
	MKA	46.14	47.45	47.19	2682.50	3457.97	3325.50	197.08	564.52	211.60
	GradMAP	46.26	50.11	47.88	72.61	42.77	82.28	190.60	447.91	198.80
	GradMAP	46.72	50.39	47.93	56.99	39.17	80.06	239.84	522.06	248.34

Table 1: Zero-shot evaluations of different pruning methods with 12.5%, 25%, and 40.63% pruning ratios across various LLMs. ‘PPL’ means perplexity on WikiText2. ‘**bold**’ indicates the best performance. – denotes models pruned using only **Stage 1** (layer selection), while – indicates models further refined by **Stage 2** (projection compensation). * denotes results reproduced by us (see Appendix D.4 for details). Pruning time in seconds.

Type	Method	Ratio	Throughput (Tokens/s)	Latency (ms)
–	Dense	0%	299 (1.00×)	1718.4 (1.00×)
Unstructured	Wanda	50%	293 (0.98×)	1555.5 (1.10×)
	SparseGPT	50%	293 (0.98×)	1555.5 (1.10×)
Structured	LLM-Pruner	20%	314 (1.05×)	1534.3 (1.12×)
	SliceGPT	20%	314 (1.05×)	1658.7 (1.04×)
	SliceGPT	25%	331 (1.11×)	1440.7 (1.19×)
	SliceGPT	30%	343 (1.15×)	1364.2 (1.26×)
Layer	GradMAP	20%	381 (1.27×)	1364.1 (1.26×)

Table 2: Throughput and latency comparison under different pruning types on LLaMA2-7B.

zero-shot evaluation, we followed standard benchmarks and assessed performance on BoolQ (Clark et al., 2019), PIQA (Bisk et al., 2020), HellaSwag(HellaS.) (Zellers et al., 2019), Winogrande(WinoG.) (Sakaguchi et al., 2021), ARC-easy (Clark et al., 2018), ARC-challenge (Clark et al., 2018), and OpenBookQA (Mihaylov et al., 2018). All compression experiments were executed on two NVIDIA A40 GPUs with 48GB. After compression, we evaluated the model on 128-token segments from WikiText2, PTB, and C4, followed by zero-shot classification on common-sense reasoning benchmarks using lm-evaluation-harness (Sutawika et al., 2023). More details about the models, datasets, training, and evaluation settings can be found in the Appendix A.

4 Main Results

Baselines. We compare our method with the following strong layer-wise compression methods:

1) **SLEB** (Song et al., 2024) prunes redundant

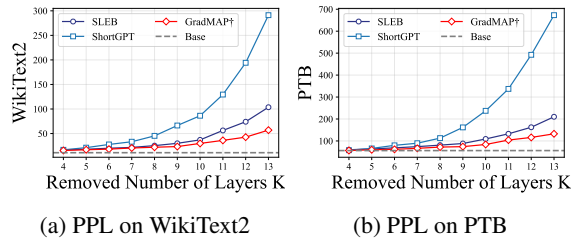


Figure 4: Perplexity of LLaMA2-7B under varying compression ratios.

blocks by leveraging output similarity between adjacent layers. During the process, each layer is sequentially masked out, and the loss metrics are calculated to evaluate its impact on model performance. This iterative layer-wise masking continues until the desired sparsity level is achieved.

2) **ShortGPT** (Men et al., 2025) employs a Block Influence (BI) metric to measure input-output similarity, identifying and removing less influential layers. The BI metric is computed for each layer of the LLM, systematically removing layers with lower scores until the model reaches the target pruning size.

3) **MKA** (Liu et al., 2024) merges similar layers via manifold learning and Normalized Pairwise Information Bottleneck alignment. Instead of direct removal, it consolidates structural knowledge, enabling hardware-friendly compression with minimal performance loss.

Zero-Shot Performance. Table 1 reports compression results across architectures on LLaMA2-7B, LLaMA2-13B, and Vicuna-7B. GradMAP

Model	Method	BoolQ \uparrow	PIQA \uparrow	HellaS. \uparrow	WinoG. \uparrow	ARC-e \uparrow	ARC-c \uparrow	OBQA \uparrow	Avg. \uparrow	Δ
LLaMA2-7B	SLEB w/ Ours Stage2	61.38 67.55	72.25 71.98	62.27 62.30	60.85 60.69	63.34 63.05	33.53 33.87	38.00 37.80	55.96 56.75	+0.79
	ShortGPT w/ Ours Stage2	53.64 58.62	68.17 68.44	62.50 62.15	65.98 65.59	55.77 56.78	34.64 34.81	38.60 38.80	54.19 55.03	+0.84
	GradMAP	70.46	70.95	63.91	65.35	64.02	37.46	38.00	58.59	–
Vicuna-7B	SLEB w/ Ours Stage2	66.64 67.37	70.29 70.35	60.17 59.53	55.96 56.27	62.54 62.25	33.79 33.62	34.80 35.40	54.88 54.97	+0.09
	ShortGPT w/ Ours Stage2	64.86 64.80	66.70 66.32	57.43 57.40	63.14 64.33	53.49 54.25	34.22 34.56	31.00 32.00	52.98 53.38	+0.40
	GradMAP	72.05	70.89	61.36	61.64	63.05	38.65	38.80	58.06	–

Table 3: Performance of integrating our projection compensation matrix with existing layer pruning methods on LLaMA2-7B and Vicuna-7B under 25% compression ratio. Δ indicates improvement after applying our Stage 2.

Model	SLEB	ShortGPT	GradMAP	GradMAP
LLaMA3.2-3B	30.10	30.46	32.69	32.75
LLaMA3.1-8B	37.62	45.50	48.68	48.92
Baichuan2-7B	32.20	38.31	39.21	39.60
Qwen2.5-7B	35.41	34.49	37.32	37.51
OPT-6.7B	36.58	29.26	37.66	38.10

Table 4: Average accuracy on more zero-shot tasks at 25% compression ratio(see Appendix E for details).

achieves a $4\times$ acceleration in pruning time on average compared to existing methods while attaining best performance across all evaluated benchmarks. Notably, while MKA prunes in similar time, its models show a severe perplexity collapse at the same compression ratios, whereas GradMAP maintains strong performance. Figure 4 shows perplexity across compression levels, where GradMAP consistently outperforms all baselines, with larger gains at higher compression ratios. To evaluate generalization, we test our framework on seven commonsense reasoning benchmarks. As shown in Table 1, GradMAP consistently outperforms all baselines across models at 25% compression, demonstrating strong effectiveness and generality. Table 4 reports the zero-shot average accuracy on Qwen2.5-7B, LLaMA3.2-3B, LLaMA3.1-8B, Baichuan2-7B, and OPT-6.7B, where GradMAP achieves the best performance. More results are provided in Appendix E.

Statistics of the Compressed Model. Table 2 summarizes the inference throughput and latency of models compressed by different pruning strategies. Unstructured pruning methods show almost no inference speedup despite high compression ratio, while structured pruning provides moderate improvements as the compression ratio increases.

Method	LLaMA2-7B	Vicuna-7B
One-Shot	50.07	50.92
GradMAP	56.08	55.88

Table 5: Ablation study of different layer selection strategies at 25% compression ratio.

In contrast, our layer pruning achieves the best efficiency, with $1.27\times$ higher throughput and $1.26\times$ lower latency at 20% compression.

Projection Compensation Matrix Seamlessly Enhances Other Layer Pruning Method. Our projection compensation matrix can be easily integrated into existing layer pruning methods to restore performance. We apply it to pruned models from several baselines and evaluate the effectiveness on the common-sense reasoning tasks. Results are shown in Table 3. After applying the projection compensation matrix, the methods show noticeable improvements. These results demonstrate the effectiveness and generalizability of our compensation approach. Notably, even with these enhancements, GradMAP still achieves superior performance, further validating the strength of our proposed metric. Furthermore, we also evaluated the memory requirements of both Stage 1 and Stage 2. Detailed results are provided in Appendix D.2 and Appendix D.3.

4.1 Ablation Study

Iterative Pruning and OneShot Pruning Analysis. We compared iterative and OneShot searches for unimportant layers in Stage 1 of GradMAP. As Table 5 shows, OneShot Pruning accelerates the process but reduces performance: for LLaMA2-7B, iterative pruning achieved 56.08% accuracy versus 50.07% with OneShot, a drop of 6.01%. We analyze that although our proposed metric can

Types	PPL \downarrow	BoolQ \uparrow	PIQA \uparrow	HellaS. \uparrow	WinoG. \uparrow	ARC-e \uparrow	ARC-c \uparrow	OBQA \uparrow	Avg. \uparrow
<i>MHA Weights</i>									
W_Q	28.49	50.98	70.73	61.17	61.80	63.01	37.80	38.20	54.81
W_K	28.49	50.98	70.73	61.17	61.80	63.01	37.80	38.20	54.81
W_V	28.54	51.65	70.51	61.10	61.80	63.09	38.31	38.20	54.95
W_O	27.94	56.36	70.67	61.00	61.72	63.09	37.88	37.40	55.45
<i>FFN Weights</i>									
W_{up}	29.05	49.63	70.18	60.77	61.96	62.58	37.46	38.00	54.37
W_{gate}	29.68	54.74	70.13	60.91	62.19	62.37	37.88	37.20	55.06
W_{down}	27.56	72.79	70.89	61.32	61.48	63.01	38.65	38.80	58.06

Table 6: Ablation of compensation on different weight matrices for Vicuna-7B at 25% compression ratio.

identify unimportant layers, the dependencies between layers in the model’s outputs require an iterative approach to update the importance scores. Since our metric is computationally efficient, the time spent remains within an acceptable range even with the iterative approach. Notably, unlike SLEB, GradMAP makes each pruning decision using a single gradient computation rather than exhaustively masking and evaluating all candidates.

The Compensation Types. We conduct an ablation study by applying the compensation module to different weight matrices in both MHA and FFN on Vicuna-7B at a 25% compression ratio (Table 6). For MHA, compensation is less effective since the projection matrices are far from the final output and involved in non-linear operations such as softmax, which limits the stability of linear compensation. In contrast, within FFN, only W_{down} provides a direct linear mapping to the output, while W_{up} and W_{gate} are embedded inside non-linear activations, making compensation unstable. Consequently, compensating W_{down} achieves the best performance, yielding the highest average accuracy across all benchmarks. Further ablation studies on compensation types, calibration data, and loss functions are in Appendix C.

5 Related Work

5.1 Traditional Pruning

Pruning has been proven to be an efficient approach for compressing pre-trained language models by removing redundant parameters (Han et al., 2016; Molchanov et al., 2019; Han et al., 2015b; He et al., 2017). Traditionally, pruning methods focused on changing weight matrices, leading to two main categories: structured pruning and unstructured pruning. Structured pruning (Ma et al., 2023; Fang et al., 2024; Zhang et al., 2023) removes

entire neurons or attention heads, while unstructured pruning (Sun et al., 2023; Frantar and Alistarh, 2023) sparsely eliminates individual weights. Despite their effectiveness, both approaches fundamentally alter the neural structure, posing significant challenges for downstream deployment due to hardware incompatibility and inference inefficiencies.

5.2 Layer Pruning

To address these limitations, layer pruning has emerged as a more flexible alternative. Recent works on layer pruning have explored various strategies in terms of importance measurement and performance recovery. For importance measurement, ShortGPT (Men et al., 2025) and Laco (Yang et al., 2024b) use cosine similarity between input and output hidden states to detect redundancy, but such methods may overlook a layers functional contribution. Loss-based methods like SLEB (Song et al., 2024) and BlockPruner (Zhong et al., 2024) address this by masking layers and measuring loss increase, albeit with high computational cost due to repeated forward passes. In summary, cosine similarity overlooks functional impact, while loss-based methods are computationally costly. Moreover, most approaches remove or merge layers without compensating for performance loss. Therefore, recent works like LLM-Streamline (Chen et al., 2024) and UIDL (Gromov et al., 2024) introduce lightweight retraining or QLoRA-based tuning to restore accuracy, but these require substantial resources. Hence, in this paper, we focus on both accurate layer importance measurement and efficient performance compensation techniques.

6 Conclusion

In this paper, we propose GradMAP, a novel layer pruning and weight compensation algorithm for LLMs. Our method leverages global gradient magnitudes to identify unimportant layers and introduces a projection compensation matrix to refine the FFN weight matrix. Extensive experiments demonstrate that GradMAP not only achieves strong performance compared to existing layer pruning methods but also accelerates the pruning process by an average factor of $4\times$.

Limitations

In this work, we propose a novel metric to evaluate the importance of layers within LLMs. By discarding unimportant layers and introducing a projection compensation matrix, we aim to mitigate the performance degradation typically associated with layer removal. While our method demonstrates superior performance compared to conventional layer pruning methods, it still falls short of the effectiveness achieved by unstructured pruning approaches at higher compression ratios. Exploring strategies to bridge this performance gap represents a promising direction for future research.

References

Josh Achiam, Steven Adler, Sandhini Agarwal, Lama Ahmad, Ilge Akkaya, Florencia Leoni Aleman, Diogo Almeida, Janko Altenschmidt, Sam Altman, Shyamal Anadkat, and 1 others. 2023. Gpt-4 technical report. *arXiv preprint arXiv:2303.08774*.

Yonatan Bisk, Rowan Zellers, Jianfeng Gao, Yejin Choi, and 1 others. 2020. Pqa: Reasoning about physical commonsense in natural language. In *Proceedings of the AAAI conference on artificial intelligence*, volume 34, pages 7432–7439.

Tom Brown, Benjamin Mann, Nick Ryder, Melanie Subbiah, Jared D Kaplan, Prafulla Dhariwal, Arvind Neelakantan, Pranav Shyam, Girish Sastry, Amanda Askell, and 1 others. 2020. Language models are few-shot learners. *Advances in neural information processing systems*, 33:1877–1901.

Xiaodong Chen, Yuxuan Hu, Jing Zhang, Yanling Wang, Cuiping Li, and Hong Chen. 2024. Streamlining redundant layers to compress large language models. *arXiv preprint arXiv:2403.19135*.

Wei-Lin Chiang, Zhuohan Li, Zi Lin, Ying Sheng, Zhanghao Wu, Hao Zhang, Lianmin Zheng, Siyuan Zhuang, Yonghao Zhuang, Joseph E Gonzalez, and 1 others. 2023. Vicuna: An open-source chatbot impressing gpt-4 with 90%* chatgpt quality, march 2023. *URL https://lmsys.org/blog/2023-03-30-vicuna*, 3(5).

Wei-Lin Chiang, Lianmin Zheng, Ying Sheng, Anastasios Nikolas Angelopoulos, Tianle Li, Dacheng Li, Hao Zhang, Banghua Zhu, Michael Jordan, Joseph E. Gonzalez, and Ion Stoica. 2024. Chatbot arena: An open platform for evaluating llms by human preference. *Preprint*, arXiv:2403.04132.

Christopher Clark, Kenton Lee, Ming-Wei Chang, Tom Kwiatkowski, Michael Collins, and Kristina Toutanova. 2019. Boolq: Exploring the surprising difficulty of natural yes/no questions. *arXiv preprint arXiv:1905.10044*.

Peter Clark, Isaac Cowhey, Oren Etzioni, Tushar Khot, Ashish Sabharwal, Carissa Schoenick, and Oyvind Tafjord. 2018. Think you have solved question answering? try arc, the ai2 reasoning challenge. *arXiv preprint arXiv:1803.05457*.

OpenCompass Contributors. 2023. Opencompass: A universal evaluation platform for foundation models. *GitHub repository*.

Tim Dettmers, Artidoro Pagnoni, Ari Holtzman, and Luke Zettlemoyer. 2023. Qlora: Efficient finetuning of quantized llms. *arXiv preprint arXiv:2305.14314*.

Gongfan Fang, Xinyin Ma, Mingli Song, Michael Bi Mi, and Xinchao Wang. 2023. Depgraph: Towards any structural pruning. In *Proceedings of the IEEE/CVF conference on computer vision and pattern recognition*, pages 16091–16101.

Gongfan Fang, Hongxu Yin, Saurav Muralidharan, Greg Heinrich, Jeff Pool, Jan Kautz, Pavlo Molchanov, and Xinchao Wang. 2024. Maskllm: Learnable semi-structured sparsity for large language models. *arXiv preprint arXiv:2409.17481*.

Elias Frantar and Dan Alistarh. 2023. Sparsegpt: Massive language models can be accurately pruned in one-shot. In *International Conference on Machine Learning*, pages 10323–10337. PMLR.

Elias Frantar, Saleh Ashkboos, Torsten Hoefer, and Dan Alistarh. 2023. Gptq: Accurate post-training quantization for generative pre-trained transformers. *International Conference on Learning Representations*.

Aaron Grattafiori, Abhimanyu Dubey, Abhinav Jauhri, Abhinav Pandey, Abhishek Kadian, Ahmad Al-Dahle, Aiesha Letman, Akhil Mathur, Alan Schelten, Alex Vaughan, and 1 others. 2024. The llama 3 herd of models. *arXiv preprint arXiv:2407.21783*.

Andrey Gromov, Kushal Tirumala, Hassan Shapourian, Paolo Glorioso, and Daniel A Roberts. 2024. The unreasonable ineffectiveness of the deeper layers. *arXiv preprint arXiv:2403.17887*.

Song Han, Huizi Mao, and William J Dally. 2016. Deep compression: Compressing deep neural networks with pruning, trained quantization and huffman coding. *International Conference on Learning Representations (ICLR)*.

Song Han, Jeff Pool, John Tran, and William Dally. 2015a. Learning both weights and connections for efficient neural network. *Advances in neural information processing systems*, 28.

Song Han, Jeff Pool, John Tran, and William Dally. 2015b. Learning both weights and connections for efficient neural network. In *Advances in Neural Information Processing Systems*, pages 1135–1143.

Yihui He, Xiangyu Zhang, and Jian Sun. 2017. Channel pruning for accelerating very deep neural networks. In *Proceedings of the IEEE international conference on computer vision*, pages 1389–1397.

Dan Hendrycks, Collin Burns, Steven Basart, Andy Zou, Mantas Mazeika, Dawn Song, and Jacob Steinhardt. 2020a. Measuring massive multi-task language understanding. *arXiv preprint arXiv:2009.03300*.

Dan Hendrycks, Collin Burns, Steven Basart, Andy Zou, Mantas Mazeika, Dawn Song, and Jacob Steinhardt. 2020b. Measuring massive multi-task language understanding. *arXiv preprint arXiv:2009.03300*.

Eldar Kurtic, Daniel Campos, Tuan Nguyen, Elias Frantar, Mark Kurtz, Benjamin Fineran, Michael Goin, and Dan Alistarh. 2022. The optimal bert surgeon: Scalable and accurate second-order pruning for large language models. *Proceedings of the 2022 Conference on Empirical Methods in Natural Language Processing*.

Guokun Lai, Qizhe Xie, Hanxiao Liu, Yiming Yang, and Eduard Hovy. 2017. Race: Large-scale reading comprehension dataset from examinations. *arXiv preprint arXiv:1704.04683*.

Hector Levesque, Ernest Davis, and Leora Morgenstern. 2012. The winograd schema challenge. In *Thirteenth international conference on the principles of knowledge representation and reasoning*.

Guangyan Li, Yongqiang Tang, and Wensheng Zhang. 2024. Lorap: Transformer sub-layers deserve differentiated structured compression for large language models. *arXiv preprint arXiv:2404.09695*.

Haonan Li, Yixuan Zhang, Fajri Koto, Yifei Yang, Hai Zhao, Yeyun Gong, Nan Duan, and Timothy Baldwin. 2023. Cmmlu: Measuring massive multitask language understanding in chinese. *arXiv preprint arXiv:2306.09212*.

Deyuan Liu, Zhanyue Qin, Hairu Wang, Zhao Yang, Zecheng Wang, Fangying Rong, Qingbin Liu, Xianchao Hao, Bo Li, Xi Chen, and 1 others. 2024. Pruning via merging: Compressing llms via manifold alignment based layer merging. In *Proceedings of the 2024 Conference on Empirical Methods in Natural Language Processing*, pages 17817–17829.

Xinyin Ma, Gongfan Fang, and Xinchao Wang. 2023. Llm-pruner: On the structural pruning of large language models. *Advances in neural information processing systems*, 36:21702–21720.

Mitch Marcus, Beatrice Santorini, and Mary Ann Marcinkiewicz. 1993. Building a large annotated corpus of english: The penn treebank. *Computational linguistics*, 19(2):313–330.

Xin Men, Mingyu Xu, Qingyu Zhang, Qianhao Yuan, Bingning Wang, Hongyu Lin, Yaojie Lu, Xianpei Han, and Weipeng Chen. 2025. Shortgpt: Layers in large language models are more redundant than you expect. In *Findings of the Association for Computational Linguistics: ACL 2025*, pages 20192–20204.

Stephen Merity, Caiming Xiong, James Bradbury, and Richard Socher. 2016. Pointer sentinel mixture models. *arXiv preprint arXiv:1609.07843*.

Todor Mihaylov, Peter Clark, Tushar Khot, and Ashish Sabharwal. 2018. Can a suit of armor conduct electricity? a new dataset for open book question answering. *arXiv preprint arXiv:1809.02789*.

Pavlo Molchanov, Arun Mallya, Stephen Tyree, Iuri Frosio, and Jan Kautz. 2019. Importance estimation for neural network pruning. In *Proceedings of the IEEE/CVF Conference on Computer Vision and Pattern Recognition*, pages 11264–11272.

Pavlo Molchanov, Stephen Tyree, Tero Karras, Timo Aila, and Jan Kautz. 2016. Pruning convolutional neural networks for resource efficient inference. *arXiv preprint arXiv:1611.06440*.

MatanBen Noach and Yoav Goldberg. 2020. Compressing pre-trained language models by matrix decomposition. *International Joint Conference on Natural Language Processing, International Joint Conference on Natural Language Processing*.

Colin Raffel, Noam Shazeer, Adam Roberts, Katherine Lee, Sharan Narang, Michael Matena, Yanqi Zhou, Wei Li, and Peter J Liu. 2020. Exploring the limits of transfer learning with a unified text-to-text transformer. *Journal of machine learning research*, 21(140):1–67.

Swarnadeep Saha, Peter Hase, and Mohit Bansal. 2023. Can language models teach? teacher explanations improve student performance via personalization. In *Thirty-seventh Conference on Neural Information Processing Systems*.

Keisuke Sakaguchi, Ronan Le Bras, Chandra Bhagavatula, and Yejin Choi. 2021. Winogrande: An adversarial winograd schema challenge at scale. *Communications of the ACM*, 64(9):99–106.

Sidak Pal Singh and Dan Alistarh. 2020. Woodfisher: Efficient second-order approximation for neural network compression. *Advances in Neural Information Processing Systems*, 33:18098–18109.

Jiwon Song, Kyungseok Oh, Taesu Kim, Hyungjun Kim, Yulhwa Kim, and Jae-Joon Kim. 2024. Sleb: streamlining llms through redundancy verification and elimination of transformer blocks. In *Proceedings of the 41st International Conference on Machine Learning*, pages 46136–46155.

Kai Sun, Dian Yu, Dong Yu, and Claire Cardie. 2020. Investigating prior knowledge for challenging chinese machine reading comprehension. *Transactions of the Association for Computational Linguistics*, 8:141–155.

Mingjie Sun, Zhuang Liu, Anna Bair, and J Zico Kolter. 2023. A simple and effective pruning approach for large language models. *arXiv preprint arXiv:2306.11695*.

Lintang Sutawika, Leo Gao, Hailey Schoelkopf, Stella Biderman, Jonathan Tow, Baber Abbasi, ben fattori, Charles Lovering, farzanehnaakhaee70, Jason Phang, Anish Thite, Fazz, Aflah, Niklas Muenighoff, Thomas Wang, sdtblck, nopperl, gakada, tt-tyuntian, and 11 others. 2023. A framework for few-shot language model evaluation.

Alon Talmor, Jonathan Herzig, Nicholas Lourie, and Jonathan Berant. 2018. Commonsenseqa: A question answering challenge targeting commonsense knowledge. *arXiv preprint arXiv:1811.00937*.

Hugo Touvron, Louis Martin, Kevin Stone, Peter Albert, Amjad Almahairi, Yasmine Babaei, NikoIay Bashlykov, Soumya Batra, Prajjwal Bhargava, Shruti Bhosale, and 1 others. 2023. Llama 2: Open foundation and fine-tuned chat models. *arXiv preprint arXiv:2307.09288*.

Ashish Vaswani, Noam Shazeer, Niki Parmar, Jakob Uszkoreit, Llion Jones, Aidan N Gomez, Łukasz Kaiser, and Illia Polosukhin. 2017. Attention is all you need. *Advances in neural information processing systems*, 30.

Thomas Wolf, Lysandre Debut, Victor Sanh, Julien Chaumond, Clement Delangue, Anthony Moi, Pieric Cistac, Tim Rault, Rémi Louf, Morgan Funtowicz, and 1 others. 2020. Transformers: State-of-the-art natural language processing. In *Proceedings of the 2020 conference on empirical methods in natural language processing: system demonstrations*, pages 38–45.

Mengzhou Xia, Zexuan Zhong, and Danqi Chen. 2022. Structured pruning learns compact and accurate models. *Proceedings of the 60th Annual Meeting of the Association for Computational Linguistics (Volume 1: Long Papers)*.

Liang Xu, Hai Hu, Xuanwei Zhang, Lu Li, Chenjie Cao, Yudong Li, Yechen Xu, Kai Sun, Dian Yu, Cong Yu, and 1 others. 2020. Clue: A chinese language understanding evaluation benchmark. *arXiv preprint arXiv:2004.05986*.

Aiyuan Yang, Bin Xiao, Bingning Wang, Borong Zhang, Ce Bian, Chao Yin, Chenxu Lv, Da Pan, Dian Wang, Dong Yan, and 1 others. 2023. Baichuan 2: Open large-scale language models. *arXiv preprint arXiv:2309.10305*.

An Yang, Baosong Yang, Beichen Zhang, Binyuan Hui, Bo Zheng, Bowen Yu, Chengyuan Li, Dayiheng Liu, Fei Huang, Haoran Wei, and 1 others. 2024a. Qwen2. 5 technical report. *arXiv preprint arXiv:2412.15115*.

Yifei Yang, Zouying Cao, and Hai Zhao. 2024b. Laco: Large language model pruning via layer collapse. In *Findings of the Association for Computational Linguistics: EMNLP 2024*, pages 6401–6417.

Zhewei Yao, Reza Yazdani Aminabadi, Minjia Zhang, Xiaoxia Wu, Conglong Li, and Yuxiong He. 2022. Zeroquant: Efficient and affordable post-training quantization for large-scale transformers. *Advances in Neural Information Processing Systems*, 35:27168–27183.

Rowan Zellers, Ari Holtzman, Yonatan Bisk, Ali Farhadi, and Yejin Choi. 2019. Hellaswag: Can a machine really finish your sentence? *arXiv preprint arXiv:1905.07830*.

Mingyang Zhang, Hao Chen, Chunhua Shen, Zhen Yang, Linlin Ou, Xinyi Yu, and Bohan Zhuang. 2023. Loraprune: Structured pruning meets low-rank parameter-efficient fine-tuning. *arXiv preprint arXiv:2305.18403*.

Chujie Zheng, Minlie Huang, and Aixin Sun. 2019. Chid: A large-scale chinese idiom dataset for cloze test. *arXiv preprint arXiv:1906.01265*.

Longguang Zhong, Fanqi Wan, Ruijun Chen, Xiaojun Quan, and Liangzhi Li. 2024. Blockpruner: Fine-grained pruning for large language models. *arXiv preprint arXiv:2406.10594*.

A Implementation Details

In this section, we provide a detailed explanation of the models we trained, evaluated, and used.

A.1 Models And Datasets

All models used in this paper are based on publicly available implementations from Hugging Face and were fine-tuned using the Hugging Face Trainer API (Wolf et al., 2020). Similarly, all datasets used for training and evaluation were downloaded directly from Hugging Face’s dataset repository. The specific models and datasets and their corresponding paths on Hugging Face are as shown in Table 7.

Models/Datasets	Repository Path
LLaMA2-7B	meta-llama/Llama-2-7b-hf
LLaMA2-13B	meta-llama/Llama-2-13b-hf
LLaMA3.1-8B	meta-llama/Llama-3.1-8B
Vicuna-7B	lmsys/vicuna-7b-v1.5
Baichuan2-7B	baichuan-inc/Baichuan2-7B-Base
OPT-6.7B	facebook/opt-6.7b
Qwen2.5-7B	Qwen/Qwen2.5-7B
WikiText2	mikasenghaas/wikitext-2
C4	allenai/c4
PTB	ptb-text-only/ptb_text_only
Bookcorpus	bookcorpus/bookcorpus
StackExchange	ArmelIR/stack-exchange-instruction
Wikipedia	wikimedia/wikipedia

Table 7: Models and Datasets Repository Information

A.2 Calibration Dataset and Training Details

In this section, we describe the details of the calibration dataset used in our experiments, as well as the hyperparameters and settings for training. The specific results are shown in Table 8. It is important to note that, for fairness, we performed re-inference and testing on the baseline models using the same calibration dataset and hyperparameters.

Seed	Tokens	Samples	Optimizer	Learning Rate	Reg Weight
42	128	128	Adam	1e-3	1e-3

Table 8: Details of the Calibration Datasets and Training Hyperparameters.

B Theoretical Analysis of Gradient-Based Metrics and Compensation

In this section, we provide theoretical insights into the effectiveness of the proposed gradient-based

layer importance evaluation and projection compensation strategy.

B.1 Gradient-Based Layer Importance

Let \mathcal{L} denote the training loss and θ_i the parameters of layer i . By the chain rule, the gradient with respect to θ_i is

$$\frac{\partial \mathcal{L}}{\partial \theta_i} = \frac{\partial \mathcal{L}}{\partial H_L} \prod_{j=i+1}^L \frac{\partial H_j}{\partial H_{j-1}} \cdot \frac{\partial H_i}{\partial \theta_i},$$

where H_j denotes the hidden states at layer j . This shows that the gradient magnitude at a layer depends both on its local Jacobian $\partial H_i / \partial \theta_i$ and the propagated sensitivity from deeper layers. Hence, the aggregated gradient norm $\|\partial \mathcal{L} / \partial \theta_i\|_2$ captures how perturbations of parameters in layer i directly affect the final loss.

Importantly, summing the norms over all tensors within the same layer (Eq. (7) in the main paper) provides a global measure of the layers sensitivity. This metric is also theoretically connected to the Fisher Information Matrix (FIM). Recall that the Fisher information of parameter θ_i is defined as

$$\mathcal{I}(\theta_i) = \mathbb{E}_{(x,y) \sim \mathcal{D}} \left[\left(\frac{\partial}{\partial \theta_i} \log p_\theta(y|x) \right)^2 \right].$$

Since the loss is the negative log-likelihood $\mathcal{L}_{CE}(x, y) = -\log p_\theta(y|x)$, we have

$$\frac{\partial \mathcal{L}_{CE}(x, y)}{\partial \theta_i} = -\frac{\partial}{\partial \theta_i} \log p_\theta(y|x),$$

which implies

$$\mathcal{I}(\theta_i) = \mathbb{E}_{(x,y) \sim \mathcal{D}} \left[\left(\frac{\partial \mathcal{L}_{CE}(x, y)}{\partial \theta_i} \right)^2 \right].$$

Therefore, the squared gradient norm provides an unbiased estimator of Fisher information. Extending this to all parameters in a layer, our score

$$s_i = \frac{1}{N} \sum_{j \in \mathcal{D}} \sum_{\theta \in \mathcal{W}_i} \left\| \frac{\partial \mathcal{L}_{CE}(\mathbf{x}^{(j)}, \mathbf{y}^{(j)})}{\partial \theta} \right\|_2.$$

directly estimates the Fisher information content of layer i .

In information-theoretic terms, Fisher information measures how sensitively the models predictive distribution depends on its parameters. Layers with higher Fisher information are more crucial for

preserving predictive accuracy. Consequently, our gradient-based score is not merely heuristic but has a principled interpretation as a Fisher information estimator, thereby providing a solid theoretical foundation for ranking layer importance.

B.2 Projection Compensation as First-Order Approximation

Pruning inevitably changes the functional mapping of the model, leading to a shift in the distribution of hidden representations. Let H_i and H'_i denote the output of layer i in the original and pruned models, respectively. For a retained layer i^* , the discrepancy can be approximated by a first-order Taylor expansion:

$$H_{i^*} \approx H'_{i^*} + J_{i^*} \Delta,$$

where J_{i^*} is the Jacobian of the transformation at layer i^* , and Δ represents the perturbation induced by pruning.

Directly computing J_{i^*} is computationally prohibitive, as it requires higher-order derivatives and large matrix operations. Instead, we approximate this correction using a learnable projection matrix W' , applied to the down-projection sub-layer. This projection acts as a low-rank surrogate for the Jacobian-based correction, aligning the pruned representation with the original one:

$$\hat{H}_{i^*} = W' W_{\text{down}}^{(i^*)} X_{\text{down}},$$

where $W_{\text{down}}^{(i^*)}$ is the original down-projection matrix and X_{down} is the input to the sub-layer. By optimizing W' under a mean-squared reconstruction loss with regularization, we ensure that \hat{H}_{i^*} approximates H_{i^*} with minimal additional complexity.

In summary, this compensation can be viewed as a constrained first-order correction: rather than re-estimating the full Jacobian, which is infeasible in practice, we introduce a parametric linear transformation that captures the dominant direction of representation drift. Thus, the projection compensation provides an efficient approximation to the local linearization of the original mapping, allowing the pruned model to preserve predictive accuracy while maintaining low computational overhead.

B.3 Comparison with Other Gradient-Based Pruning Methods

While gradients have been explored in prior pruning works, their roles and targets differ substan-

tially from our approach. For example, DepGraph (Fang et al., 2023) employs gradients primarily for optimization during iterative sparse training, while its final pruning criterion remains norm-based (e.g., L_2 magnitude). Similarly, LLM-Pruner (Ma et al., 2023) employs gradients only at a fine granularity, directly pruning individual neurons or attention heads without capturing higher-level structural importance.

In contrast, GradMAP directly uses global gradient magnitudes as a sensitivity metric to assess importance without parameter updates. More importantly, our method is explicitly designed for *layer-level* pruning, enabling the identification of functionally redundant blocks rather than individual low-magnitude weights. This distinction allows GradMAP to translate importance estimation into practical inference acceleration, as reflected by the consistent throughput and latency gains.

C More Ablation Studies

Model	\mathcal{L}_{MSE}	\mathcal{L}_{reg}	Avg.↑
LLaMA2-7B	✓	✗	56.54
	✗	✓	56.66
	✓	✓	58.59
Vicuna-7B	✓	✗	56.98
	✗	✓	55.32
	✓	✓	58.15

Table 9: Ablation of loss functions.

C.1 The Impact of Loss Function

In this section, we perform an ablation study on the loss components of our projection compensation matrix learning by analyzing the individual contributions of the mean squared error (MSE) loss and the regularization term in our objective function. The quantitative results are presented in Table 9. Our findings indicate that using MSE loss alone leads to severe overfitting on the calibration dataset, as the model fails to generalize beyond the limited 128 calibration samples. On the other hand, relying solely on regularization loss fails to provide meaningful performance improvements, as the projection compensation matrix lacks sufficient adaptation to the pruned model. At the 25.00% compression ratio on Vicuna-7B, using only MSE loss yields 56.98% accuracy, and only regularization loss gives 55.32%. In contrast, our combined loss achieves 58.15%, outperforming MSE by 2.0% and regularization by 5.1%.

Model	Dataset	PIQA↑	HellaS.↑	WinoG.↑	ARC-e↑	ARC-c↑	Avg.↑
LLaMA3.1-8B	Wikipedia	73.23	69.69	71.11	67.34	44.80	65.23
	C4	72.03	70.33	71.27	66.67	45.56	65.17
	WikiText2	73.45	69.44	69.69	70.29	44.71	65.52
	StackExchange	73.45	71.36	71.19	68.56	44.45	65.80
	Bookcorpus	73.94	70.90	71.43	66.84	43.86	65.39
Baichuan2-7B	Wikipedia	71.00	63.76	67.09	64.10	36.09	60.40
	C4	70.78	62.73	67.25	63.22	38.31	60.45
	WikiText2	70.35	65.38	67.42	63.76	37.80	60.94
	StackExchange	70.40	64.44	67.96	61.45	37.80	60.41
	Bookcorpus	70.40	64.44	67.96	61.45	37.80	60.41

Table 10: Model performance with different datasets used as calibration data.

This highlights the effectiveness of our loss design in stabilizing pruned model performance. Therefore, we adopt a balanced combination of MSE and regularization to ensure effective weight adaptation and model robustness after pruning.

Model	Type	Time↓	Accuracy↑
LLaMA2-7B	Right	1475.1	58.70
	Left	54.0	58.59
LLaMA2-13B	Right	2758.3	59.48
	Left	93.1	59.49
Vicuna-7B	Right	1487.2	58.05
	Left	80.6	58.15

Table 11: Comparison of different calibration types on zero-shot performance.

C.2 The Impact of Calibration Type

In this section, we investigate different strategies for applying the projection compensation matrix. Specifically, we examine the effects of either left-multiplying or right-multiplying the down-projection matrix within the FFN. The results of these two approaches are summarized in Table 11.

For the weight matrix, we denote its dimension as $\mathbf{W}^{(i^*)} \in \mathbb{R}^{d \times k}$, with the condition that $k \gg d$. Consequently, training a left-multiplying projection compensation matrix requires learning parameters in a matrix of dimension $\mathbf{W}_{\text{left}}' \in \mathbb{R}^{d \times d}$, whereas a right-multiplying projection compensation matrix necessitates training parameters in a matrix of dimension $\mathbf{W}_{\text{right}}' \in \mathbb{R}^{k \times k}$. Therefore, employing a left-multiplying projection compensation matrix significantly reduces computational overhead, leading to faster and more efficient training. Experimental results corroborate this efficiency, demonstrating that utilizing a left-multiplying projection compensation matrix main-

tains model performance while achieving a **20-fold** increase in calibrating speed.

Method	LLaMA2-7B	Vicuna-7B
Local	56.66	55.57
Top-5	57.95	56.31
Top-2	58.21	57.70
GradMAP	58.59	58.15

Table 12: Ablation study of the compensation strategies.

C.3 The Impact of Calibration Data

In this section, we analyze the impact of calibration data by selecting several common calibration datasets. Each dataset contains 128 randomly selected samples, with each sample having a token length of 128. We conducted experiments using the LLaMA2-7B model, and the results are presented in Table 10. From these results, we observe similar performance post-pruning across different calibration datasets, demonstrating the robustness of ours metrics.

C.4 The Different Compensation Strategies

We examined two strategies: local compensation, which adjusts neighboring layer weights (e.g., updating layer 2 when layer 3 is pruned), and GradMAP, which identifies layers with the largest output shifts through a one-time analysis and selectively adjusts them. As Table 12 shows, GradMAP substantially improves performance. Ablation on Top- Z shift layers reveals diminishing or negative returns as Z increases, likely due to overfitting limited calibration data and eroding pre-trained knowledge, while larger Z adds unnecessary computation. We therefore adopt a minimal strategy, adjusting only the most drifted layer.

Method	LLaMA2-7B	LLaMA2-13B	LLaMA3.1-8B	Vicuna-7B	Baichuan2-7B
SLEB	10,26,22,13,14,15,24	19,14,8,10,33,27,31,28,22,26	22,11,23,10,28,20,9,7	11,24,28,21,8,7,27,12	22,11,23,10,28,20,9,7
ShortGPT	25,24,27,23,26,28,21	31,29,30,28,27,26,24,22,23,19	25,24,23,22,21,20,19,18	25,24,23,21,19,18,17,16	25,24,23,22,21,20,19,18
GradMAP	27,25,24,12,23,13,21	32,29,22,35,14,30,27,13,34,28	26,23,25,22,20,28,10,19	27,25,24,12,23,21,13,11	26,23,25,22,20,28,10,19

Table 13: Pruned layer indices selected by different methods across various models.

Model	Compress Ratio	GPU	#GPU	Memory Usage (MB)	Running Time (s)
LLaMA2-7B	25.00%	NVIDIA A40(48G)	1	13674	123.42
Vicuna-7B	25.00%	NVIDIA A40(48G)	1	13674	148.63
LLaMA3.1-8B	25.00%	NVIDIA A40(48G)	1	15810	144.54
Baichuan2-7B	25.00%	NVIDIA A40(48G)	1	16374	140.71
OPT-6.7B	25.00%	NVIDIA A40(48G)	1	12712	161.38
LLaMA2-13B	25.00%	NVIDIA A40(48G)	1	26706	299.30

Table 14: Comparison of GPU Memory Usage and Running Time of The Stage 1

Model	Compress Ratio	GPU	#GPU	Memory Usage (MB)	Running Time (s)
LLaMA2-7B	25.00%	NVIDIA A40(48G)	1	16342	46.0
Vicuna-7B	25.00%	NVIDIA A40(48G)	1	16418	45.5
LLaMA3.1-8B	25.00%	NVIDIA A40(48G)	1	19154	49.1
Baichuan2-7B	25.00%	NVIDIA A40(48G)	1	17524	47.8
OPT-6.7B	25.00%	NVIDIA A40(48G)	1	16308	48.2
LLaMA2-13B	25.00%	NVIDIA A40(48G)	1	29342	69.0

Table 15: Comparison of GPU Memory Usage and Running Time of The Stage 2

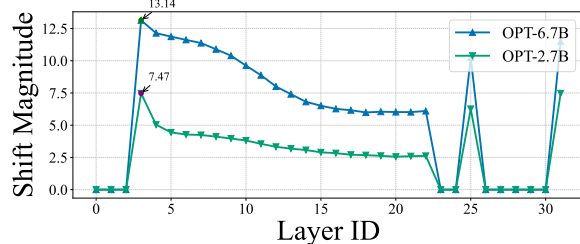


Figure 5: Distribution of first-order moment offsets before and after pruning for OPT-6.7B and OPT-2.7B.

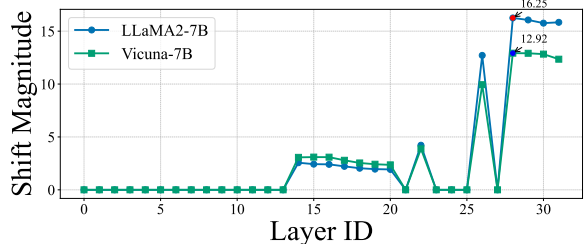


Figure 6: Distribution of first-order moment offsets before and after pruning for LLaMA2-7B and Vicuna-7B.

C.5 Layer-Wise Shift and Compensation Analysis

We conducted a visual analysis of the first-order moment for retained layers across different models before and after pruning. The results are illustrated in Figure 6 and Figure 5. We observed an intriguing phenomenon regarding the locations of maximum shift magnitudes across different model architectures. As illustrated in Figure 6, for LLaMA2-7B and Vicuna-7B, the shift magnitudes gradually increase as layers are pruned; however, a decreasing trend emerges in the final layers, with the maximum offsets appearing notably at the (N-3)-th layer. In contrast, Figure 5 shows that for the OPT model family, the shift magnitudes exhibit a consistent pattern of first increasing and then decreasing throughout the middle layers, with their

peak occurring distinctly at the third layer. These findings highlight model differences in parameter sensitivities and suggest considerations for optimizing pruning strategies across various LLMs.

D More Experiments

D.1 Pruned Layers Across Different LLMs

In this section, we present the pruned layer selections of different models under various pruning methods. The detailed results are summarized in Table 13.

D.2 Memory Usage and Running Time of Stage 1

In this section, we evaluate the computational resources required for Stage 1 of GradMAP. As shown in Table 14, the memory usage across

Method	Removed Layers	PPL (WikiText2)↓	Pruning Time (s)
ShortGPT-OneShot	21,22,23,24,25,26,27,28	NaN (Collapse)	145.95
ShortGPT-Iterative	25,24,23,21,19,18,17,16	48.37	923.20
SLEB	11,24,28,21,8,7,27,12	31.66	902.32
GradMAP	27,25,24,12,23,21,13,11	28.49	148.63

Table 16: Comparison of ShortGPT pruning strategies on Vicuna-7B.

Method	MMLU↑	CMMLU↑	GSM8k↑	XSum↑	StrategyQA↑	Avg.↑
SLEB	25.42	22.36	0.89	0.15	18.47	13.46
ShortGPT	28.59	40.62	7.89	1.67	20.13	19.78
GradMAP	30.77	48.89	11.45	1.67	40.74	26.70
GradMAP	30.17	51.84	11.51	2.12	40.79	27.20

Table 17: Performance comparison on additional datasets and generative tasks using Baichuan2-7B.

all models remains relatively low, with even the largest model (LLaMA2-13B) consuming only about 26 GB of GPU memory. In terms of running time, Stage 1 is highly efficient: most models complete the process in under 2.5 minutes, and smaller models (e.g., 7B variants) typically finish within 1 minutes. This demonstrates that Stage 1 is lightweight in both memory and time, making it practical and easy to deploy in real-world scenarios.

D.3 Memory Usage and Runing Time of Stage 2

In this section, we analyze the computational resources required for Stage 2 of GradMAP, with the results summarized in Table 15. As shown, all models complete this stage in under one minute using a single NVIDIA A40 GPU. The memory footprint remains moderate, with 7B-scale models requiring less than 20 GB of GPU memory. Even for larger models like LLaMA2-13B, the memory usage stays within 30 GB, and the runtime remains efficient at 69 seconds. These results confirm that Stage 2 is highly resource-efficient and easily deployable in practice.

D.4 Reproduction of ShortGPT

We reproduce ShortGPT following the one-shot layer pruning strategy described in the paper. In our experiments on Vicuna-7B, we observe that one-shot pruning often selects consecutive intermediate layers, which significantly disrupts feature propagation and leads to model collapse at higher pruning ratios. Table 16 reports the empirical comparison. When removing 8 layers,

the original ShortGPT-OneShot strategy results in NaN perplexity on WikiText2, indicating an invalid model. To obtain a valid and comparable baseline, we further implement an iterative pruning variant, where layer importance scores are recomputed after each pruning step. This strategy effectively avoids model collapse and yields finite perplexity.

For fair comparison under functional model settings, the results reported for ShortGPT in the main experiments correspond to this reproduced ShortGPT-Iterative configuration.

D.5 Results on Generative and Reasoning Tasks

To further demonstrate the robustness and generalization of our method, we additionally evaluate GradMAP on several reasoning and generative benchmarks, including GSM8k, XSum, and StrategyQA, using Baichuan2-7B as the backbone model. These tasks cover diverse evaluation settings, ranging from mathematical reasoning to abstractive summarization and strategic question answering.

Table 17 summarizes the performance comparison with representative baselines. Overall, GradMAP consistently achieves strong performance across all tasks.

E More Results

In this section, we follow the evaluation setup proposed by LLM-Streamline (Chen et al., 2024) and adopt OpenCompass (Contributors, 2023) to conduct a comprehensive assessment across a broader range of models and benchmarks.

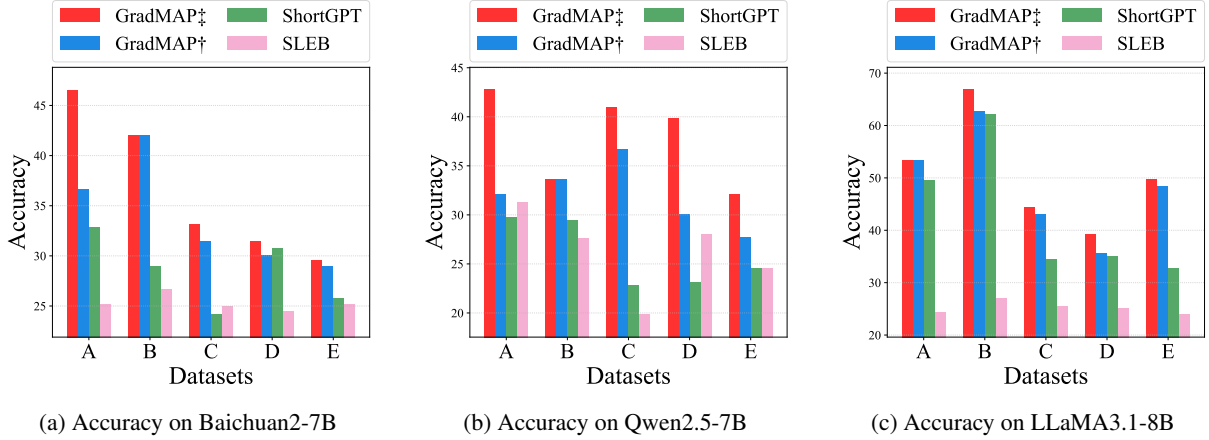


Figure 7: Accuracy comparison on different CMMLU dataset subjects during pruning. The subjects include: A: Chinese Driving Rule, B: Legal and Moral Basis, C: Professional Psychology, D: High School Politics, E: Economics.

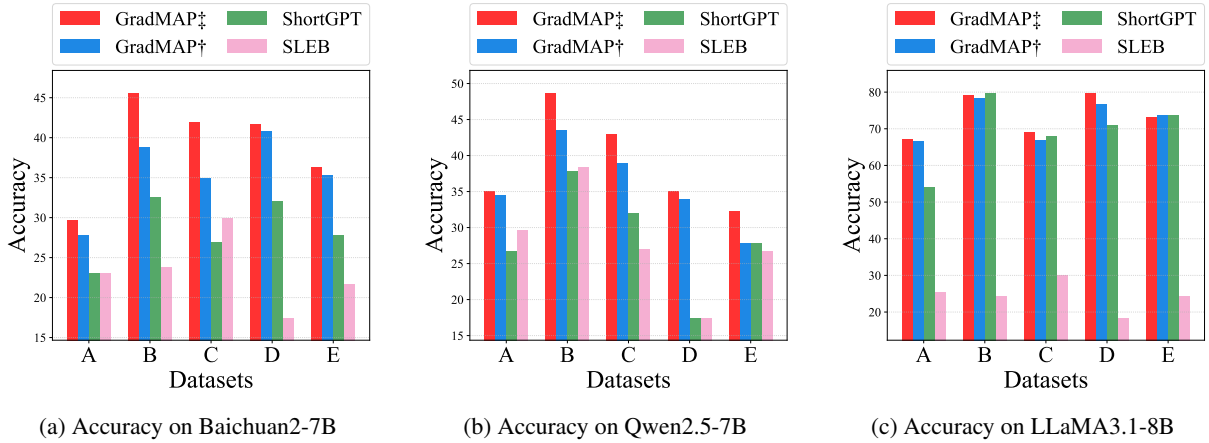


Figure 8: Accuracy comparison on different MMLU dataset subjects during pruning. Subjects: A: High School European History, B: High School Government and Politics, C: Medical Genetics, D: Management, E: High School Geography.

Specifically, under the OpenCompass framework, we extend our evaluation by incorporating 12 additional benchmarks covering natural language understanding and question-answering tasks: C3 (Sun et al., 2020), CMNLI (Xu et al., 2020), CHID (Zheng et al., 2019), BoolQ (Clark et al., 2019), WSC (Levesque et al., 2012), HellaSwag (HeSW) (Zellers et al., 2019), PIQA (Bisk et al., 2020), Race-High/Middle (Lai et al., 2017), MMLU (Hendrycks et al., 2020b), CMMLU (Li et al., 2023) and CommonSenseQA (CoQA) (Talmor et al., 2018).

E.1 Results on MMLU Subjects and CMMLU Subjects

In this section, we conduct Zero-Shot evaluations on specific tasks from the MMLU and CMMLU benchmarks using Baichuan2-7B, Qwen2.5-7B

and LLaMA3.1-8B models. The results are presented in Figure 7 and Figure 8. As illustrated, our proposed GradMAP consistently achieves superior performance across the evaluated tasks.

E.2 Results on LLaMA3.1-8B

We conduct detailed experiments on LLaMA3.1-8B to evaluate the effectiveness of different pruning strategies. As shown in Table 18, our method GradMAP consistently outperforms all baselines across various compression ratios. Notably, it maintains competitive perplexity and zero-shot accuracy, indicating a better trade-off between compression and performance retention.

E.3 Results on Baichuan2-7B

In this section, we evaluate the pruning performance on the Baichuan2-7B model. Table 19

demonstrates that GradMAP achieves the best results in terms of both perplexity and zero-shot downstream accuracy. These results highlight the generalizability of our approach across model families beyond the LLaMA series.

E.4 Results on OPT-6.7B

We also test our approach on the OPT-6.7B model to verify its robustness on non-Transformer-based model variants. As presented in Table 20, GradMAP still outperforms other methods, achieving lower perplexity and higher downstream accuracy under various compression settings. This demonstrates the broad applicability of GradMAP across diverse model architectures.

Model	Method	Ratio	Benchmarks												Average
			C3	CMNLI	CHID	BoolQ	WSC	HeSW	PIQA	CoQA	Race-M	Race-H	MMLU	CMMLU	
LLaMA3.1-8B	Dense	0.00%	54.08	32.98	36.99	69.79	71.10	74.66	80.96	71.42	70.61	63.15	66.74	50.87	59.07
	SLEB	25.0%	37.15	33.10	11.79	54.43	62.50	48.96	70.46	39.72	21.31	21.38	25.29	25.29	37.62
	ShortGPT	25.0%	43.23	<u>33.13</u>	7.09	57.86	63.50	55.71	69.21	54.22	35.17	<u>35.17</u>	56.69	35.12	45.50
	GradMAP	25.0%	<u>47.07</u>	32.72	<u>26.07</u>	53.15	63.50	<u>58.54</u>	73.45	59.13	<u>40.60</u>	35.48	54.98	<u>39.60</u>	48.68
	GradMAP	25.0%	47.67	33.43	26.97	53.79	<u>62.50</u>	60.05	<u>72.91</u>	58.72	40.74	33.85	<u>55.63</u>	40.77	48.92

Table 18: Accuracy of different pruning methods across classification benchmarks on LLaMA3.1-8B.

Model	Method	Ratio	Benchmarks												Average
			C3	CMNLI	CHID	BoolQ	WSC	HeSW	PIQA	CoQA	Race-M	Race-H	MMLU	CMMLU	
Baichuan2-7B	Dense	0.00%	62.41	33.28	9.59	62.94	66.65	64.33	74.59	66.00	50.77	52.20	54.68	56.91	53.20
	SLEB	25.0%	39.18	31.70	<u>11.59</u>	38.29	60.58	30.59	57.73	22.28	21.38	25.27	25.42	22.36	32.20
	ShortGPT	25.0%	<u>47.45</u>	<u>33.53</u>	5.49	54.71	65.38	46.56	62.68	23.26	24.50	27.00	28.59	40.62	38.31
	GradMAP	25.0%	46.58	33.37	10.94	<u>43.88</u>	<u>63.46</u>	<u>50.53</u>	66.49	22.91	23.84	28.92	30.77	<u>48.89</u>	<u>39.21</u>
	GradMAP	25.0%	49.70	33.64	12.89	41.96	62.50	51.16	<u>66.21</u>	<u>23.12</u>	<u>24.47</u>	<u>27.54</u>	<u>30.17</u>	51.84	39.60

Table 19: Accuracy of different pruning methods across classification benchmarks on Baichuan2-7B.

Model	Method	Ratio	Benchmarks												Average
			C3	CMNLI	CHID	BoolQ	WSC	HeSW	PIQA	CoQA	Race-M	Race-H	MMLU	CMMLU	
OPT-6.7B	Dense	0.00%	37.86	32.83	13.14	64.04	66.35	62.77	75.73	56.92	25.63	25.81	24.82	25.33	41.04
	SLEB	25.0%	35.56	32.80	0.00	45.63	63.46	50.88	72.25	42.18	22.77	<u>23.79</u>	24.40	25.25	36.58
	ShortGPT	25.0%	25.97	32.89	0.05	45.14	56.73	26.33	53.10	17.61	22.28	22.16	23.63	<u>25.24</u>	29.26
	GradMAP	25.0%	<u>36.11</u>	<u>32.96</u>	<u>2.90</u>	<u>59.76</u>	<u>64.42</u>	49.36	68.01	<u>38.82</u>	25.63	24.24	<u>24.67</u>	25.03	<u>37.66</u>
	GradMAP	25.0%	36.16	32.97	7.09	60.61	65.38	49.78	<u>68.39</u>	38.33	<u>25.49</u>	23.38	24.74	24.87	38.10

Table 20: Accuracy of different pruning methods across classification benchmarks on OPT-6.7B.